Supplemental Information

Emerging Indoor Photovoltaics for Self-Powered and Self-Aware IoT towards Sustainable Energy Management

Hannes Michaels[a,†], Michael Rinderle[b,†], Richard Freitag[b,c], Iacopo Benesperi[a], Alessio Gagliardi[b], and Marina Freitag[a,*]

[a] School of Natural and Environmental Science, Bedson Building, Newcastle University, NE1 7RU, Newcastle upon Tyne, UK
[b] TUM School of Computation, Information and Technology, Technical University of Munich, Hans-Piloty-Straße 1, 85748, Garching, Germany
[c] Swedish University Network (Sunet), Tulegatan 11, 113 53 Stockholm, Sweden
[†] These authors contributed equally
[*] Corresponding author: marina.freitag@newcastle.ac.uk

Indoor photovoltaic cells and IoT device tests

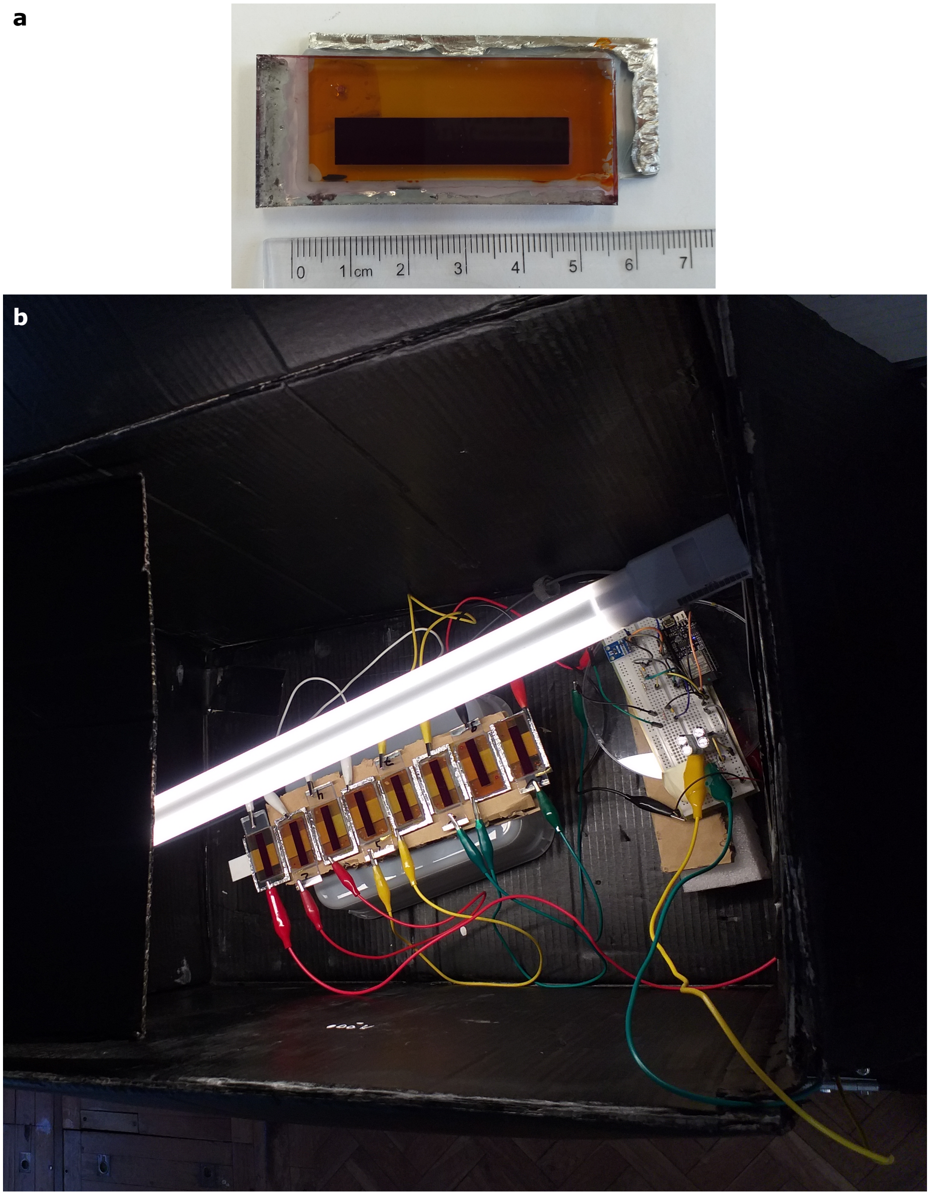

Figure S1: Photographs of **a**, a 3.2 cm^2 XY1:L1-sensitised photovoltaic cell and **b**, a test setup powering a ESP32-FireBeetle-based IoT sensor device with ambient light harvested by photovoltaic cells.

Osram Warm White 930 fluorescent light tube

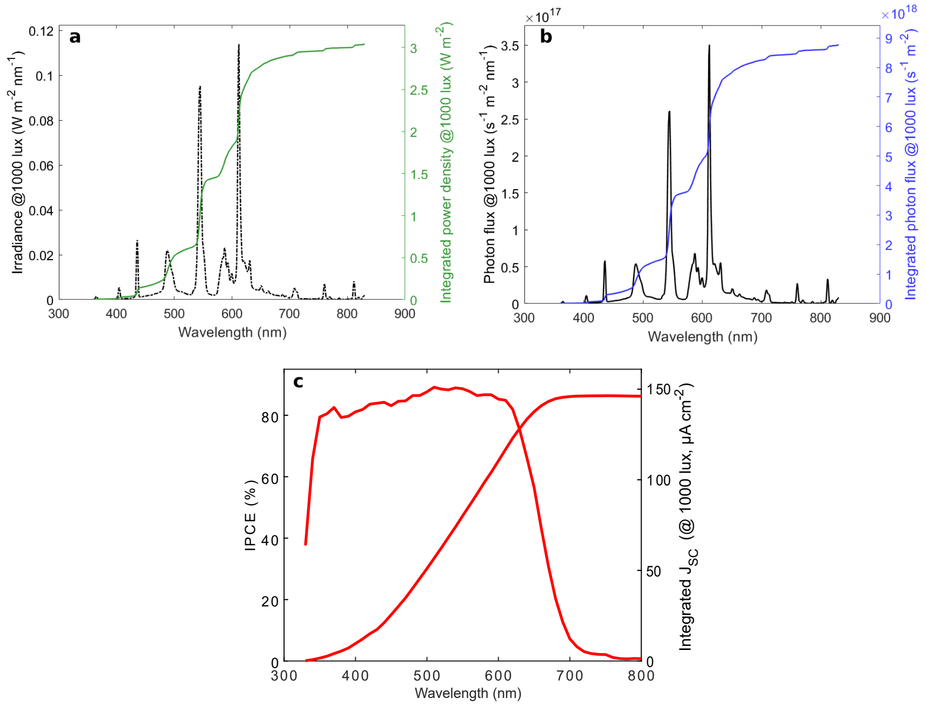

Figure S2: Characterisation of the Osram Warm White 930 fluorescent light tube. **a**, lamp spectrum (in power density) and integrated available power. **b**, emission spectrum (in photon flux) and integrated available photons. **c**, External quantum efficiency spectrum and integrated photocurrent.

Overview of IoT operation scenarios

Table S1: Deployment scenarios for the wireless IoT devices powered by indoor photovoltaic cells.

Scenario	Setting	Light spectrum	Max. lux	Min. lux
Factory	controlled	fluorescent tube	1000	1000
Office	controlled	fluorescent tube	1000	0
Home	fluctuating	fluorescent tube + natural light	$\sim$5000	800

Overview of DSC electrolyte compositions

Table S2: Electrolyte compositions in the tested DSCs.

Description	Redox mediator	Cu^{II} concentration (M)	Lewis base
$Cu(tmby)_2$ NMBI 0.1 M Cu^{II}	$Cu(tmby)_2$	0.1	NMBI
$Cu(tmby)_2$ NMBI 0.06 M Cu^{II}	$Cu(tmby)_2$	0.06	NMBI
$Cu(tmby)_2$ NMBI 0.02 M Cu^{II}	$Cu(tmby)_2$	0.02	NMBI
$Cu(tmby)_2$ *t*BP 0.06 M Cu^{II}	$Cu(tmby)_2$	0.06	*t*BP
$Cu(dmby)_2$ NMBI 0.06 M Cu^{II}	$Cu(dmby)_2$	0.06	NMBI

$Cu(tmby)_2$: bis-(4,4',6,6'-tetramethyl-2,2'-bipyridine)copper(II/I) bis(trifluoromethanesulfonyl)imide
$Cu(dmby)_2$: bis-(6,6'-dimethyl-2,2'-bipyridine)copper(II/I) bis(trifluoromethanesulfonyl)imide
NMBI: *N*-methyl benzimidazole
*t*BP: *tert*-butyl pyridine

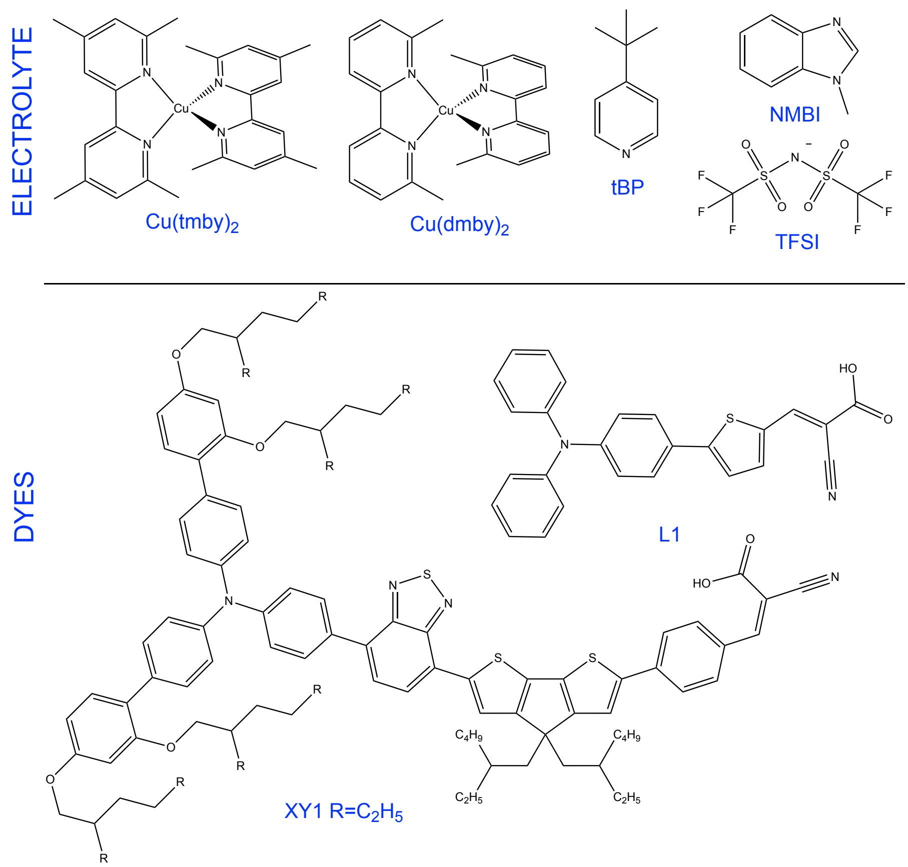

Figure S3: Chemical structures of coordination complexes, counter ions, organic dyes and Lewis bases used in the DSCs.

Characterisation of photovoltaic cells under one-sun AM1.5G.

Table S3: Performance metrics of XY1:L1-sensitised photovoltaic cells under one-sun AM1.5G irradiation, by electrolyte composition.

	Voc (V)	Jsc (μA cm^{-2})	FF	PCE (%)
$Cu(tmby)_2$ NMBI 0.1 M Cu^{II}	1.04 1.04 ± 0.02	13.6 13.2 ± 0.45	0.750 0.739 ± 0.013	10.4 10.1 ± 0.23
$Cu(tmby)_2$ NMBI 0.06 M Cu^{II}	1.07 1.06 ± 0.02	12.7 12.2 ± 0.47	0.705 0.708 ± 0.012	9.47 9.17 ± 0.30
$Cu(tmby)_2$ NMBI 0.02 M Cu^{II}	1.00 1.02 ± 0.02	12.4 12.0 ± 0.41	0.640 0.609 ± 0.024	7.94 7.47 ± 0.28
$Cu(tmby)_2$ *t*BP 0.06 M Cu^{II}	1.07 1.05 ± 0.02	12.6 12.3 ± 0.31	0.770 0.769 ± 0.008	10.4 10.0 ± 0.31
$Cu(dmby)_2$ NMBI 0.06 M Cu^{II}	1.03 1.04 ± 0.02	12.1 12.2 ± 0.27	0.685 0.657 ± 0.017	8.56 8.37 ± 0.23

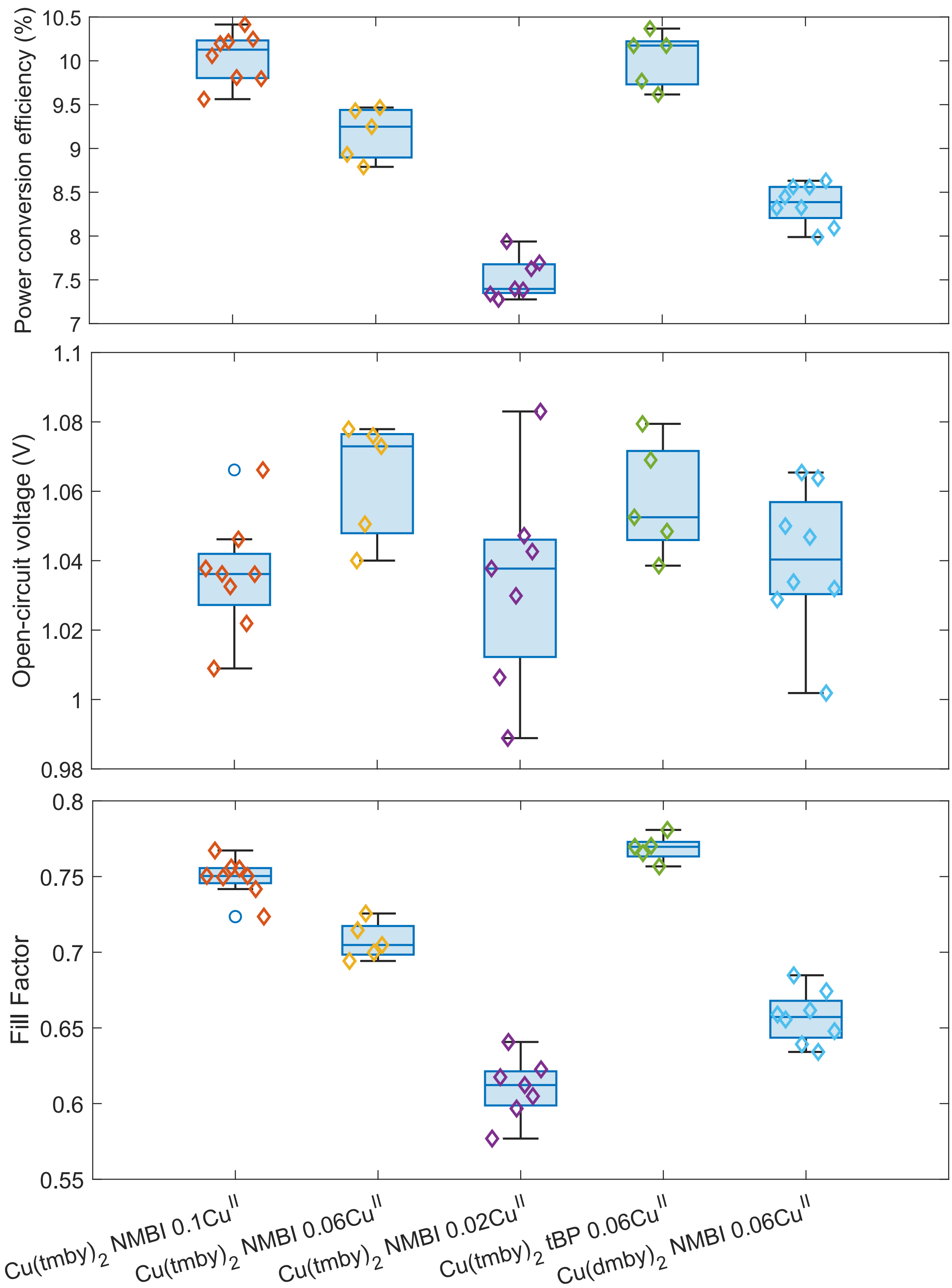

Figure S4: Performance metrics of XY1:L1-sensitised photovoltaic cells under one-sun AM1.5G irradiation, by electrolyte composition.

Characterisation of photovoltaic cells under 0.5 sun irradiation.

Table S4: Performance metrics of XY1:L1-sensitised photovoltaic cells under 0.5 sun irradiation, by electrolyte composition.

	Voc (V)	Jsc (μA cm^{-2})	FF	PCE (%)
$Cu(tmby)_2$ NMBI 0.1 M Cu^{II}	1.00 1.00 ± 0.01	6.91 6.64 ± 0.28	0.773 0.777 ± 0.005	10.6 10.3 ± 0.26
$Cu(tmby)_2$ NMBI 0.06 M Cu^{II}	1.02 1.03 ± 0.01	6.80 6.67 ± 0.11	0.754 0.740 ± 0.012	10.5 10.2 ± 0.29
$Cu(tmby)_2$ NMBI 0.02 M Cu^{II}	1.03 1.04 ± 0.02	6.18 6.04 ± 0.21	0.639 0.645 ± 0.008	8.15 8.14 ± 0.10
$Cu(tmby)_2$ *t*BP 0.06 M Cu^{II}	1.01 1.01 ± 0.01	6.83 6.63 ± 0.18	0.790 0.800 ± 0.010	10.9 10.7 ± 0.18
$Cu(dmby)_2$ NMBI 0.06 M Cu^{II}	1.00 1.01 ± 0.02	6.65 6.53 ± 0.18	0.731 0.719 ± 0.017	9.61 9.51 ± 0.12

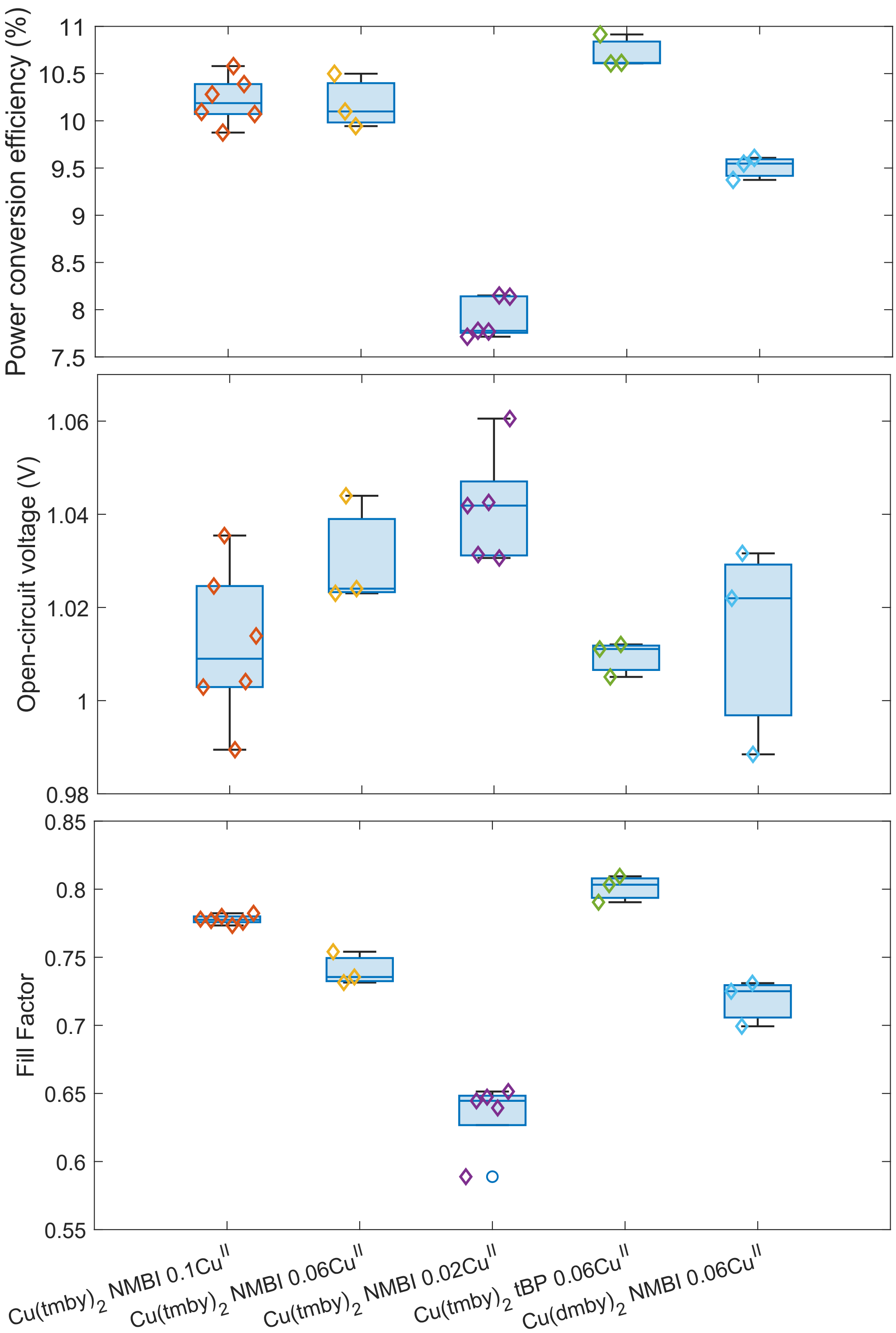

Figure S5: Performance metrics of XY1:L1-sensitised photovoltaic cells under 0.5 sun irradiation, by electrolyte composition.

Characterisation of photovoltaic cells under 0.14 sun irradiation.

Table S5: Performance metrics of XY1:L1-sensitised photovoltaic cells under 0.14 sun irradiation, by electrolyte composition.

	Voc (V)	Jsc (μA cm^{-2})	FF	PCE (%)
$Cu(tmby)_2$ NMBI 0.1 M Cu^{II}	0.985 0.966 ± 0.011	1.89 1.88 ± 0.01	0.802 0.794 ± 0.007	10.5 10.1 ± 0.26
$Cu(tmby)_2$ NMBI 0.06 M Cu^{II}	1.00 0.999 ± 0.007	1.93 1.92 ± 0.02	0.780 0.776 ± 0.007	10.8 10.6 ± 0.20
$Cu(tmby)_2$ NMBI 0.02 M Cu^{II}	0.986 0.986 ± 0.024	1.92 1.82 ± 0.06	0.740 0.698 ± 0.030	9.70 8.95 ± 0.58
$Cu(tmby)_2$ *t*BP 0.06 M Cu^{II}	0.975 0.975 ± 0.004	1.92 1.91 ± 0.01	0.790 0.794 ± 0.011	10.6 10.4 ± 0.29
$Cu(dmby)_2$ NMBI 0.06 M Cu^{II}	0.950 0.973 ± 0.021	1.94 1.82 ± 0.10	0.755 0.755 ± 0.009	10.1 9.55 ± 0.656

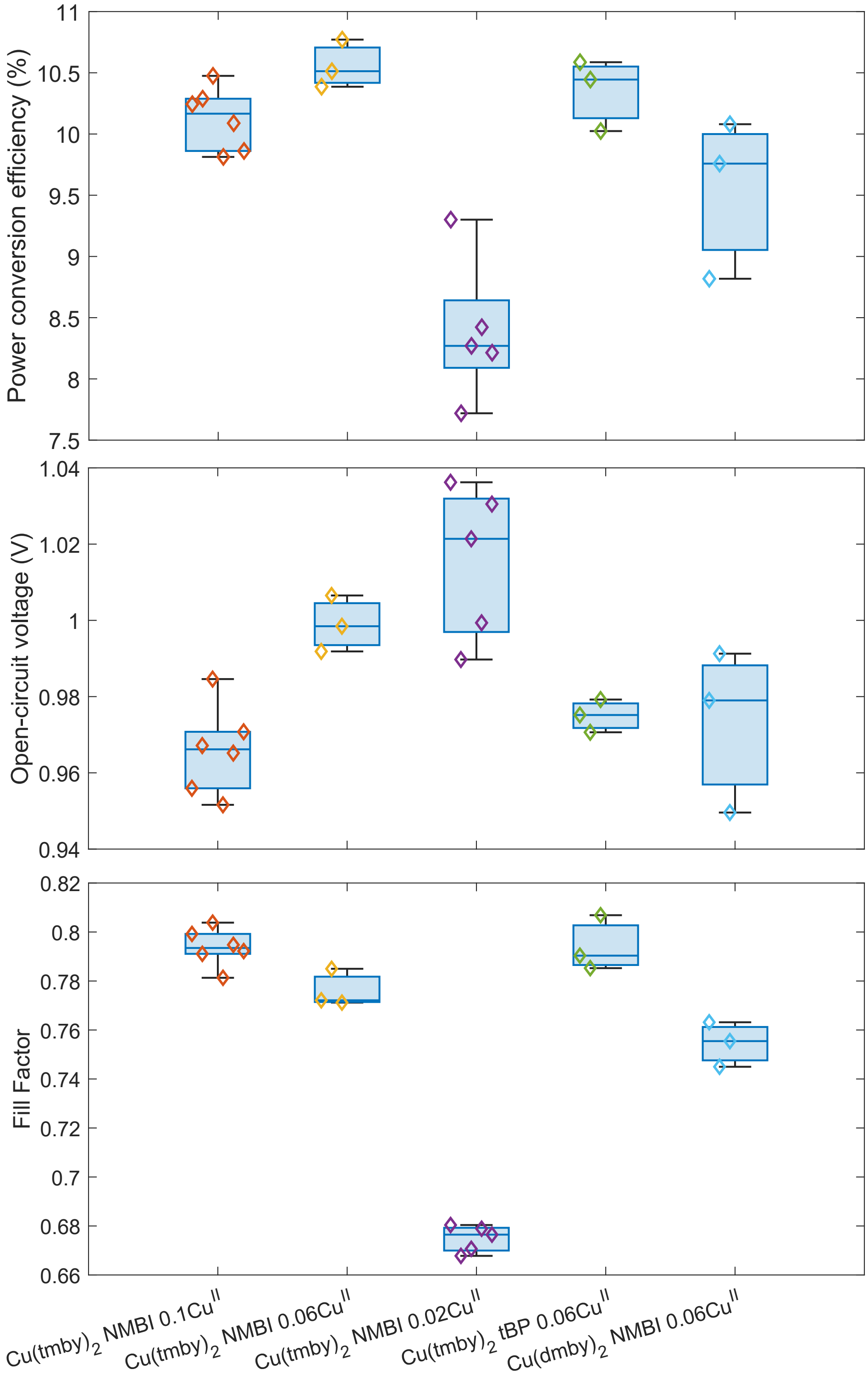

Figure S6: Performance metrics of XY1:L1-sensitised photovoltaic cells under 0.14 sun irradiation, by electrolyte composition.

Characterisation of photovoltaic cells under ambient light.

Table S6: Performance metrics of XY1:L1-sensitised photovoltaic cells at 1000 lux ambient illumination (fluorescent lamp), by electrolyte composition.

	Voc (V)	Jsc (μA cm^{-2})	FF	PCE (%)
$Cu(tmby)_2$ NMBI 0.1 M Cu^{II}	0.916 0.915 ± 0.006	147 -from IPCE-	0.808 0.801 ± 0.008	36.0 35.7 ± 0.34
$Cu(tmby)_2$ NMBI 0.06 M Cu^{II}	0.995 0.974 ± 0.014	147 -from IPCE-	0.778 0.790 ± 0.002	37.5 36.9 ± 0.47
$Cu(tmby)_2$ NMBI 0.02 M Cu^{II}	1.00 1.00 ± 0.02	145 145 ± 1	0.726 0.730 ± 0.004	35.1 34.8 ± 0.60
$Cu(tmby)_2$ *t*BP 0.06 M Cu^{II}	0.952 0.953 ± 0.006	147 -from IPCE-	0.782 0.780 ± 0.009	36.0 35.6 ± 0.39
$Cu(dmby)_2$ NMBI 0.06 M Cu^{II}	0.970 0.945 ± 0.035	139 138 ± 1	0.769 0.777 ± 0.019	34.1 33.5 ± 0.66

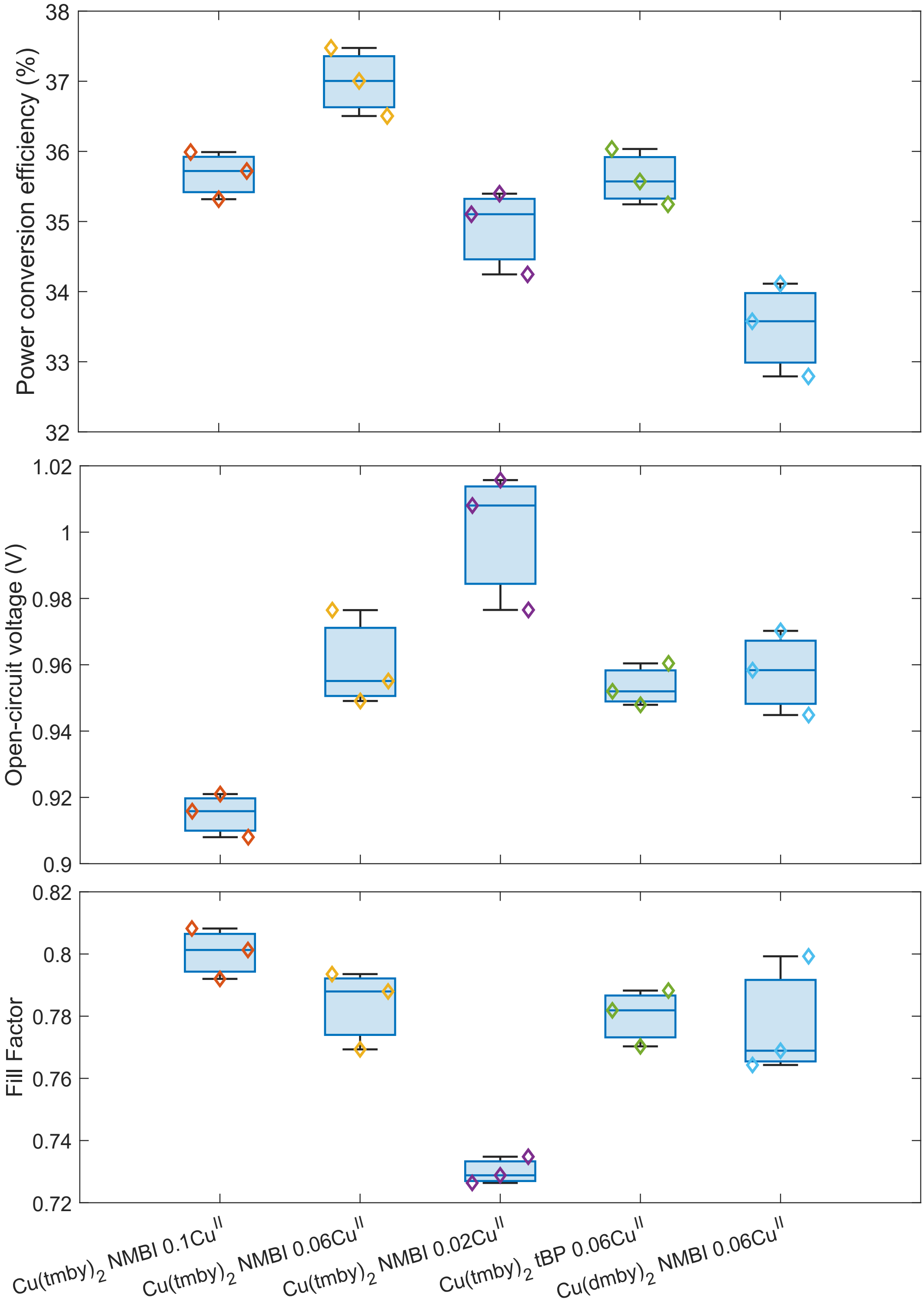

Figure S7: Performance metrics of XY1:L1-sensitised photovoltaic cells at 1000 lux ambient illumination (fluorescent lamp), by electrolyte composition.

Observations on current-voltage hysteresis.

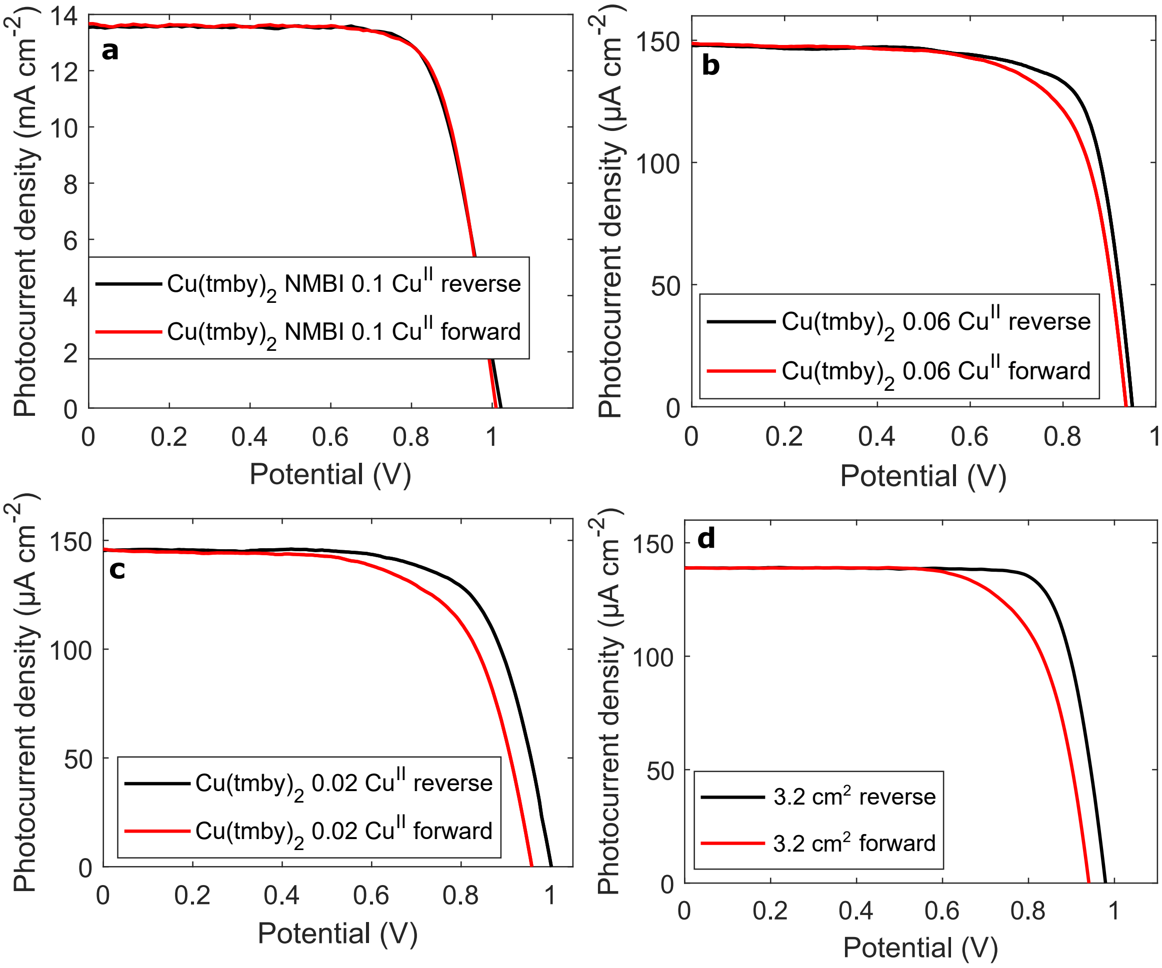

Figure S8: Current-voltage hysteresis of XY1:L1-sensitised photovoltaic cells, by electrolyte composition. **a**, 0.384 cm^2 cell comprising 0.1 M Cu^{II} at one sun. **b**, 0.384 cm^2 cell comprising 0.06 M and **c**, 0.02 M Cu^{II} at 1 000 lux ambient light (fluorescent lamp). **d**, 3.2 cm^2 cell (comprising 0.06 M Cu^{II}) at 1 000 lux. Performance metrics are listed in Tabs. S7-S10.

Table S7: Performance metrics of a 0.384 cm^2 cell comprising 0.1 M Cu^{II} at one-sun; HI = 0.

	Voc (V)	Jsc (μA cm-2)	FF	PCE (%)
reverse	1.02	13.6	0.750	10.4
forward	1.01	13.7	0.751	10.4

Table S8: Performance metrics of a 0.384 cm^2 cell comprising 0.06 M Cu^{II} at 1000 lux indoor illumination; HI = 0.031.

	Voc (V)	Jsc (μA cm-2)	FF	PCE (%)
reverse	0.955	147	0.788	36.3
forward	0.945	147	0.713	34.1

Table S9: Performance metrics of a 0.384 cm^2 cell comprising 0.02 M Cu^{II} at 1000 lux indoor illumination; HI = 0.060.

	Voc (V)	Jsc (μA cm-2)	FF	PCE (%)
reverse	1.00	145	0.726	35.1
forward	0.962	145	0.678	31.1

Table S10: Performance metrics of a 3.2 cm^2 cell comprising 0.06 M Cu^{II} at 1000 lux indoor illumination; HI = 0.092

	Voc (V)	Jsc (μA cm-2)	FF	PCE (%)
reverse	0.984	139	0.821	37.1
forward	0.948	139	0.688	30.8

Characterisation under ambient light

Table S11: Performance metrics of a 3.2 cm^2 cell comprising 0.06 M Cu^{II}, by illumination intensity.

	Voc (V)	Jsc (μA cm-2)	FF	PCE (%)
1000 lux	0.984	139	0.821	37.1
500 lux	0.950	69.7	0.800	34.8
200 lux	0.919	27.6	0.812	33.7

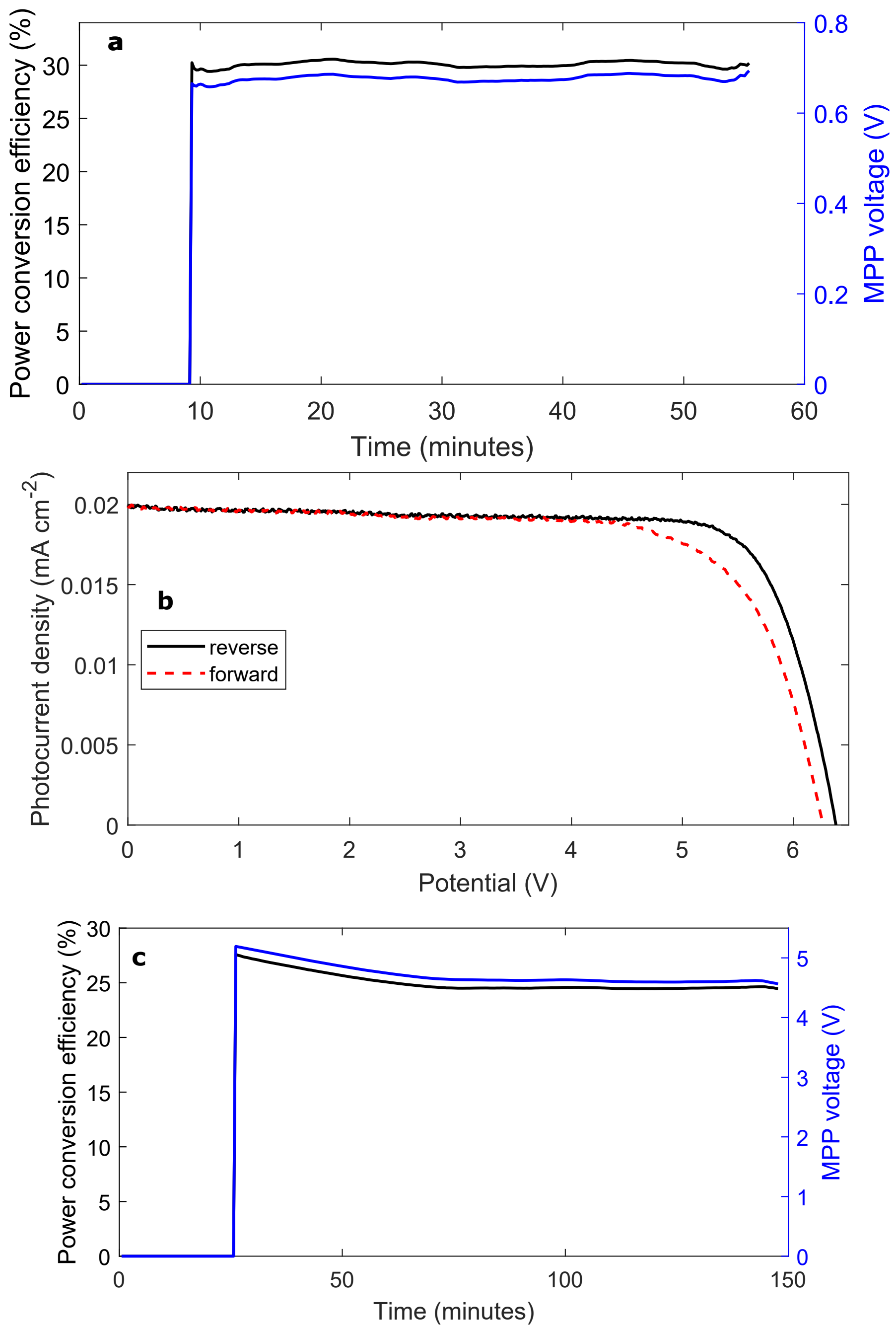

Figure S9: **a**, MPP tracking of 3.2 cm^2 cell at 1 000 lux illumination; stabilised PCE 30.3%, V_{MPP} 0.678 V. **b**, $J-V$ sweep (Performance metrics in Tab. S12) and **c**, maximum power point tracking of an array of seven 3.2 cm^2 cells (total area 22.4 cm^2), stabilised PCE 27.5%, V_{MPP} 4.62 V.

Table S12: Performance metrics of an array of seven 3.2 cm^2 cells (total area 22.4 cm^2); corresponding to Fig. S9.

	Voc (V)	Jsc (µA cm-2)	FF	PCE (%)
reverse	6.385	20	0.772	32.5
forward	6.267	20	0.708	29.1

Transient photovoltage

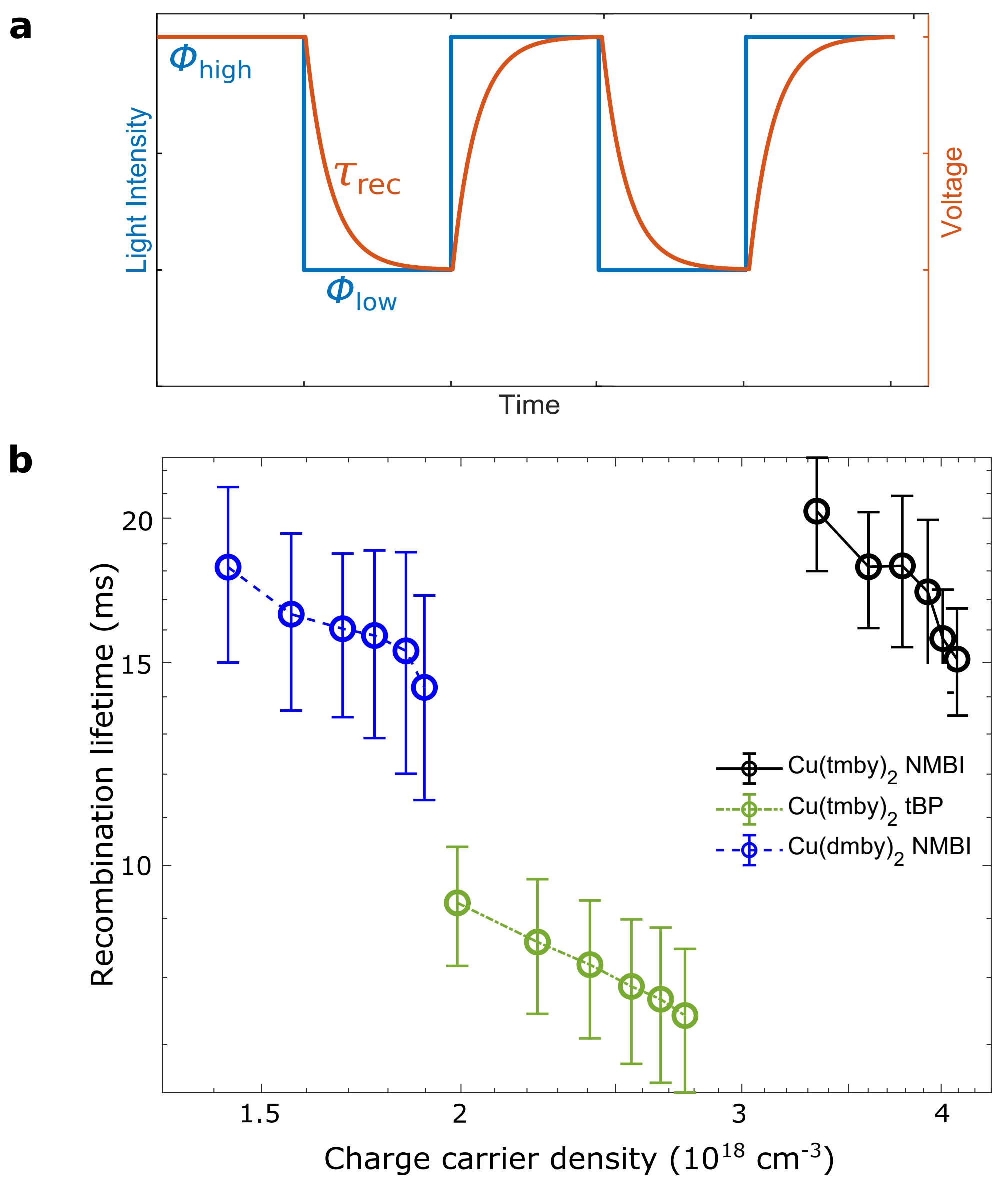

Figure S10: Electron recombination lifetime probed by transient photovoltage.

Sensitiser regeneration

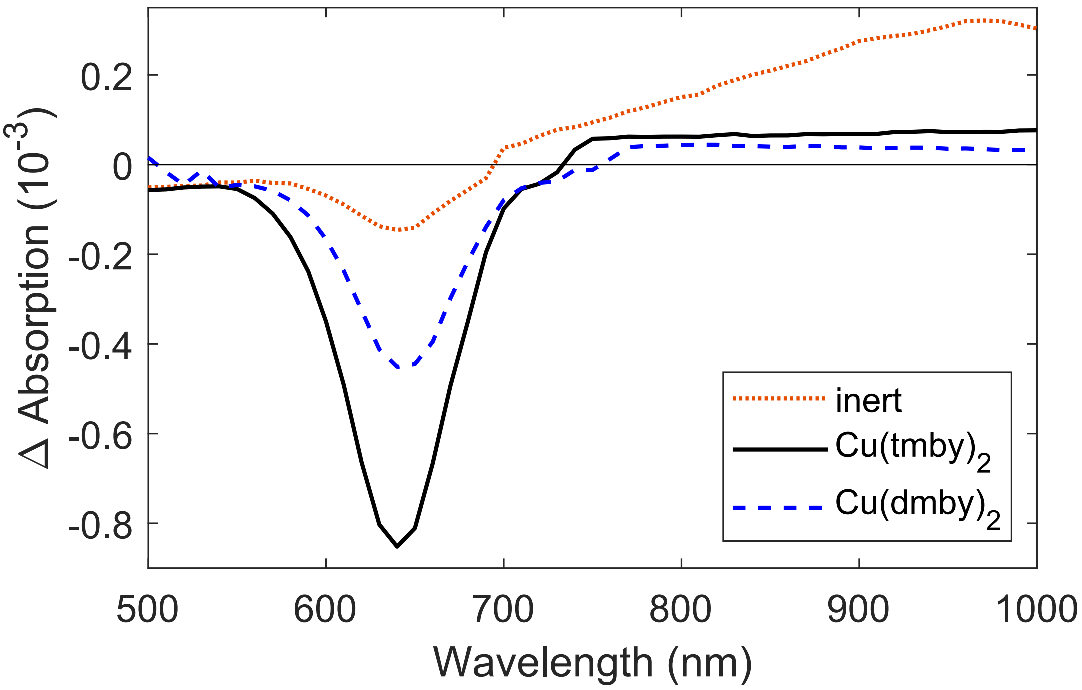

Figure S11: Sensitiser regeneration probed by photoinduced absorption spectroscopy. The XY1 dye is regenerated rapidly by both the $Cu(tmby)_2$ and $Cu(dmby)_2$ redox mediator.

Ambient-Light-powered electronic devices

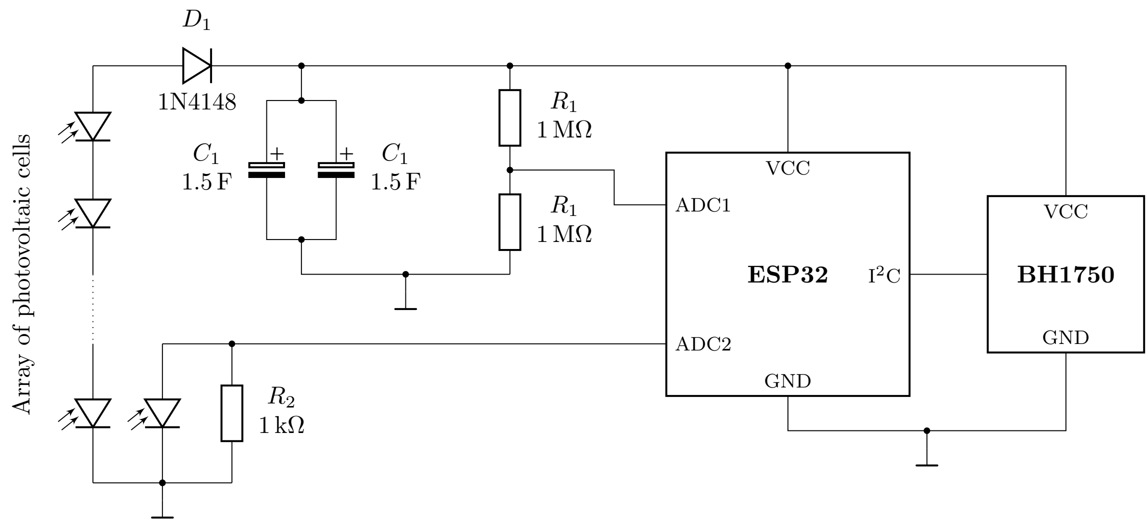

Figure S12: Schematic of the energy harvesting sensor system based on the FireBeetle ESP32 microcontroller. The system is powered by an array of photovoltaic cells. To buffer energy for dark times, two supercapacitors C_1 are used. Diode D_1 prevents the supercapacitors from discharging through the photovoltaic cells. A voltage divider made of the two resistors R_1 is used to measure the capcacitor voltage and prevents the ADC1 pin from voltages above 3.3 V. The cell current is measured on an additional photovoltaic cell in parallel to the supply array. The lux sensor BH1750 is connected to the microcontroller via the I^{2}C-bus.

Pseudocode

```
setup                                             // Initial microcontroller setup
    Configure ADC
    Configure BH1750 lux meter
    if first boot then
        establish WiFi connection
        Synchronize clock via NTP
        disconnect WiFi
    end if
end setup

loop                                              // Start microcontroller loop
    V_c ← Cap voltage measurement from ADC1
    if V_c < 2.9 then
        goto deep sleep
    end if
    I_c ← Cell current measurement from ADC2
```

```
    lx ← Illumination measurement from BH1750
    t ← Timestamp
    scenario ← LSTM_PREDICTION(lx)
    advance measurement counter

    if persistent buffer not full then
        append measurement to buffer
    else
        if V_c < 3.3 then                      // Voltage too low to safely start WiFi
            store persistent buffer in flash memory
            clear persistent buffer
        else                                   // Voltage high enough for WiFi
            establish WiFi connection
            send measurements from flash memory via TCP
            send measurements from persistent buffer via TCP
            disconnect WiFi
            clear flash memory
            clear persistent buffer
        end if
    end if

    if scenario is 0 then                      // Run scenario dependent workload
        run office workload
    else if scenario is 1 then
        run factory workload
    else if scenario is 2 then
        run home workload
    else
        no prediction available
    end if
    goto sleep
end loop
```

Data time series from light-powered ESP32 sensor devices

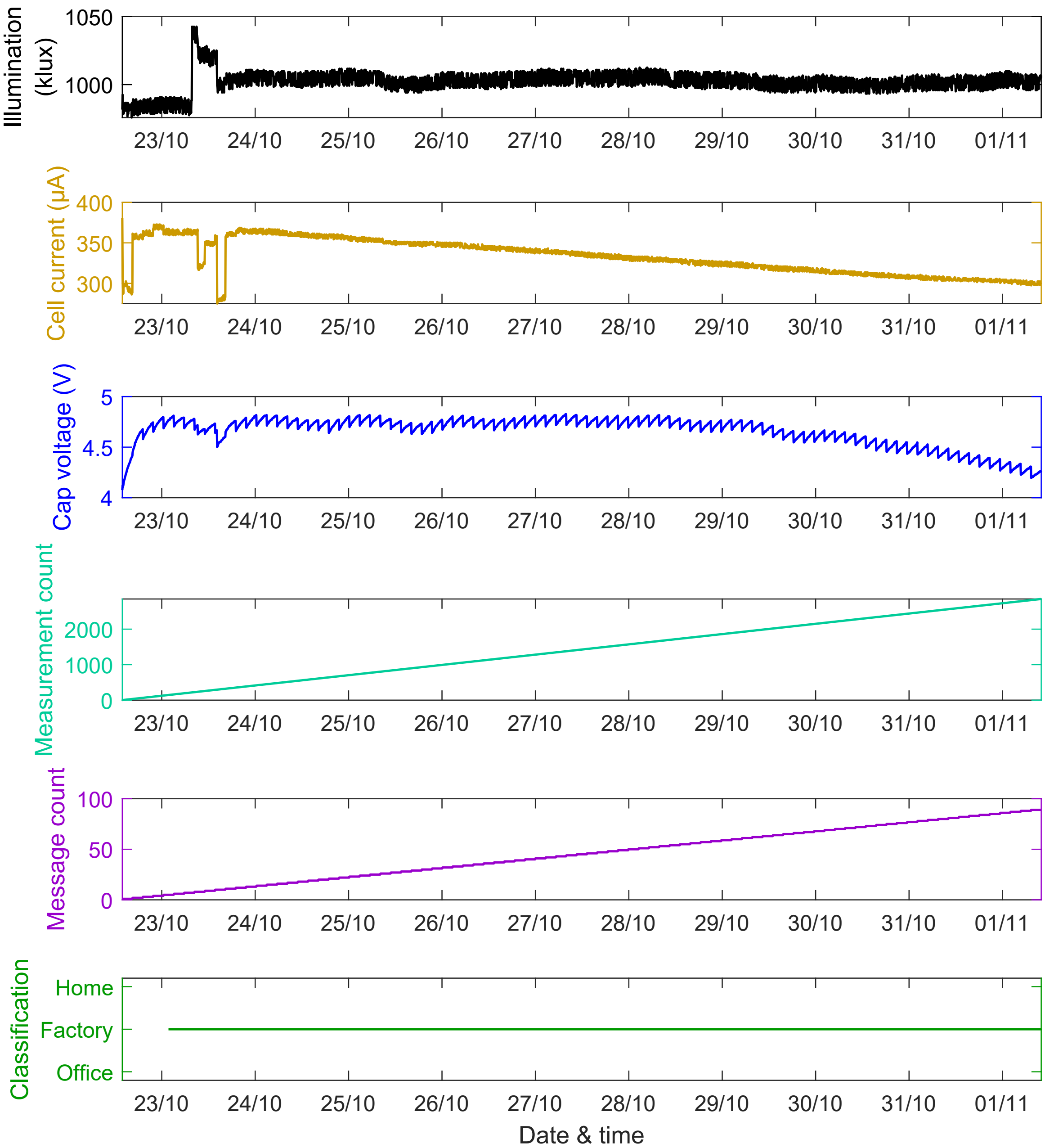

Figure S13: Time series data from a ESP32 FireBeetle microcontroller, powered an array of seven 3.2 cm^2 cells (total area 22.4 cm^2), in the *factory* setting. The recorded data include illumination, cell photocurrent, capacitor voltage, number of measurements, number of transmitted packages, as well as the categorisation of the deployment scenario based on the pre-trained artificial neural network.

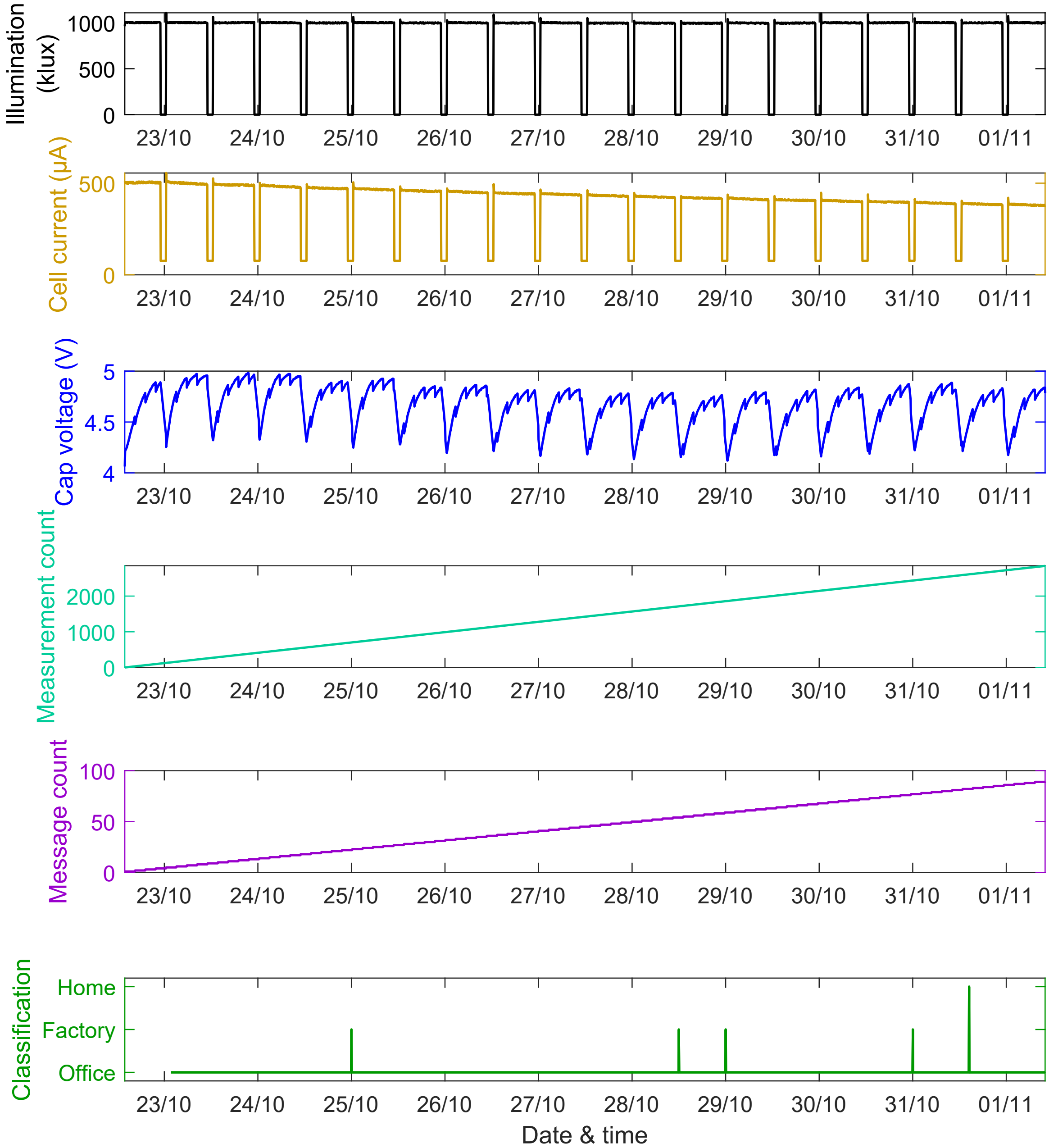

Figure S14: Time series data from a ESP32 FireBeetle microcontroller, powered an array of seven $3.2\,\text{cm}^2$ cells (total area $22.4\,\text{cm}^2$), in the *office* setting. The recorded data include illumination, cell photocurrent, capacitor voltage, number of measurements, number of transmitted packages, as well as the categorisation of the deployment scenario based on the pre-trained artificial neural network.

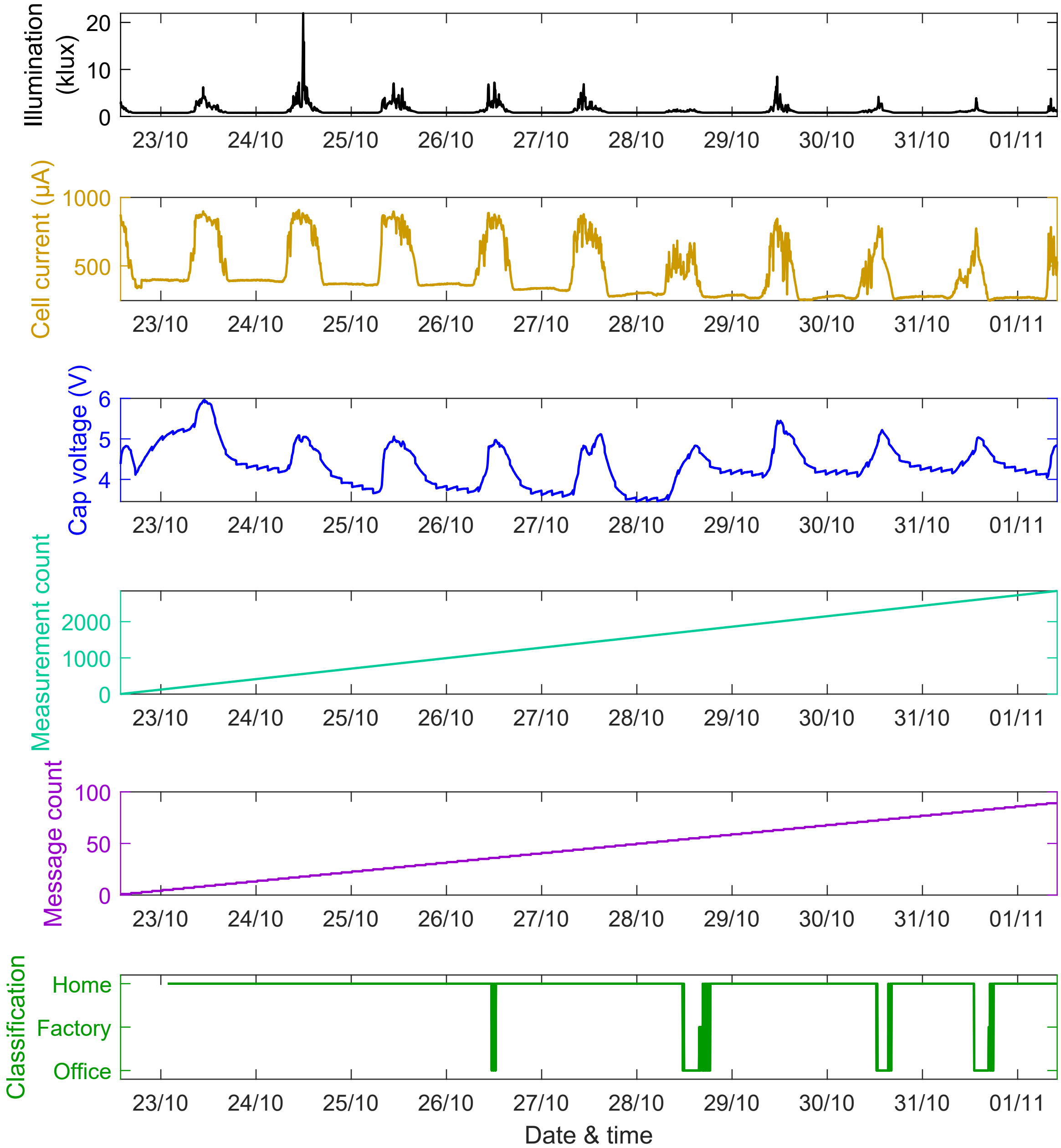

Figure S15: Time series data from a ESP32 FireBeetle microcontroller, powered an array of seven $3.2\,cm^2$ cells (total area $22.4\,cm^2$), in the *home* setting. The recorded data include illumination, cell photocurrent, capacitor voltage, number of measurements, number of transmitted packages, as well as the categorisation of the deployment scenario based on the pre-trained artificial neural network.